

Josephson Effect

Michael Schmid* and Henri Menke†

Gruppe M05, Fortgeschrittenenpraktikum, University of Stuttgart
(February 2, 2015)

Superconductivity is the phenomenon of electric current being transported without any losses. In this experiment we study a specific feature of superconductors called *Josephson effect*. We determine the Stewart-McCumber parameter and the peak Josephson current density of the Niob tunnelling junction as well as the London penetration depth. Furthermore the dependency of the Josephson current on the temperature and the magnetic field is determined.

BASICS

The Josephson effect derives from a certain property of special materials called superconductors. Before we dive into the description of the Josephson effect we settle the features of superconductivity.

Superconductivity

There exist certain materials which, when they are cooled below a specific critical temperature, lose their resistance with respect to the transport of electric current. Because the resistance of a superconducting material exhibits a sharp edge at the jump temperature the superconducting state qualifies as a physical phase. Superconductivity is a phase transition of second order.

Macroscopic Interpretation: An ideal conductor, if placed in a weak external magnetic field \mathbf{B} and cooled down, is flooded with the magnetic field. A superconductor in contrast ejects the field up to a certain depth called the London penetration depth λ . The field inside of the superconductor can be expressed by

$$\mathbf{B}_i = \mu_0(\mathbf{H} + \mathbf{M}) = \mu_0(\mathbf{H} + \chi\mathbf{H}) = \mu_0\mathbf{H}(1 + \chi) \quad (1)$$

with the magnetic field constant μ_0 , the magnetic field intensity \mathbf{H} and the susceptibility χ . The susceptibility χ determines the characteristics of the respective material, viz. $\chi < 0$ is called *diamagnetic*, $\chi > 0$ is called *paramagnetic*. For $\chi = -1$, i.e. vanishing inner field we speak about an ideal diamagnet.

Quantum Mechanical Interpretation: During the measurement of tiny screening currents it was found that they are quantised with $h/(2e)$. This means that a quantum theory is needed to fully understand the phenomenon of superconductivity. It was found that an attractive interaction between electrons emerges in the superconducting phase. This interaction is communicated via the exchange of a virtual phonon in the lattice of the superconductor. More intuitively, an electron polarises the lattice and the emerging positive charge cloud attracts another electron.

London Equations

In the macroscopic interpretation it is possible to derive effective equations which describe the dynamics of the supercurrent. For the London equations it is assumed that the superconducting charges obey a modified version of Ohm's law where not the current density but its temporal derivative is proportional to the electric field. Thus for $\mathbf{E} = 0$ one has $\partial_t \mathbf{j} = 0$ which implies $\mathbf{j} = \text{const}$, that is a current will also flow without an external field. The London equations read with the index S standing for *superconducting*

$$\mathbf{j}_S = \frac{n_S e_S^2}{m_S} \mathbf{E} \quad 1. \text{ London equation} \quad (2)$$

$$\nabla \times \mathbf{j}_S = -\frac{n_S e_S^2}{m_S} \mathbf{B} \quad 2. \text{ London equation} \quad (3)$$

where n_S is the particle density, e_S the charge of the superconducting charges and m_S their mass.

Because screening currents require the presence of a magnetic field the external field has to penetrate a little. Consider therefore $\nabla \times \mathbf{B} = \mu_0 \mathbf{j}_S$

$$\nabla \times (\nabla \times \mathbf{B}) = -\nabla^2 \mathbf{B} = \mu_0 \nabla \times \mathbf{j}_S \quad (4)$$

with the second London equation

$$\nabla^2 \mathbf{B} = \frac{\mu_0 n_S e_S^2}{m_S} \mathbf{B} \quad (5)$$

Using an ansatz of an exponential decay $\mathbf{B} = B_0 e^{-x/\lambda_L}$ and $\mathbf{j}_S = j_{S,0} e^{-x/\lambda_L}$ yields

$$\lambda_L = \sqrt{\frac{m_S}{\mu_0 n_S e_S^2}} \quad (6)$$

This quantity is called the London penetration depth and is in general of the order 15 nm.

From the London equation we can immediately draw conclusions for a microscopic theory. We know that we can obtain an electric and a magnetic field from the vector potential \mathbf{A}

$$\mathbf{B} = \text{rot } \mathbf{A}, \quad \mathbf{E} = -\frac{\partial \mathbf{A}}{\partial t}. \quad (7)$$

In Coulomb gauge one has

$$\operatorname{div} \mathbf{A} = 0 . \quad (8)$$

We plug this into the material equations where we abbreviate $\Lambda = m_S / (n_S e_S^2)$.

$$\Lambda \frac{\partial \mathbf{j}_S}{\partial t} = - \frac{\partial \mathbf{A}}{\partial t} \quad (9)$$

$$\Lambda \operatorname{rot} \mathbf{j}_S = - \operatorname{rot} \mathbf{A} \quad (10)$$

From these two equations we find by comparison (or integration)

$$\Lambda \mathbf{j}_S = - \mathbf{A} . \quad (11)$$

To gain a better insight into the meaning of this expression we consider the definition of the probability flux density of quantum theory. With minimal coupling to the magnetic field one has

$$\mathbf{j}(\mathbf{x}) = \underbrace{\frac{e\hbar}{2mi} [\psi^*(\mathbf{x}) \nabla \psi(\mathbf{x}) - \psi(\mathbf{x}) \nabla \psi^*(\mathbf{x})]}_{\mathbf{j}_1} - \underbrace{\frac{e^2}{m} \mathbf{A} \psi^*(\mathbf{x}) \psi(\mathbf{x})}_{\mathbf{j}_2} . \quad (12)$$

In term of the field quantisation one obviously has to replace $\psi^*(\mathbf{x})$ and $\psi(\mathbf{x})$ with the respective field operators $\hat{\psi}^\dagger(\mathbf{x})$ and $\hat{\psi}(\mathbf{x})$. Thus $\mathbf{j}(\mathbf{x})$ also becomes an operator $\hat{\mathbf{j}}(\mathbf{x})$, which possesses an expectation value.

$$\langle \hat{\mathbf{j}}(\mathbf{x}) \rangle = \langle \Phi | \hat{\mathbf{j}}(\mathbf{x}) | \Phi \rangle . \quad (13)$$

If there is no vector potential \mathbf{A} present, i.e. no magnetic field, the flux density vanishes in the ground state, because the expression \mathbf{j}_1 in square brackets is zero. If the expression in brackets \mathbf{j}_1 were still zero when a magnetic field is present then $\Lambda \mathbf{j}_S = - \mathbf{A}$ would be fulfilled. In this case the flux density would reduce to

$$\langle \hat{\mathbf{j}}(\mathbf{x}) \rangle = - \frac{e^2}{m} \mathbf{A} \langle \Phi | \hat{\psi}^\dagger(\mathbf{x}) \hat{\psi}(\mathbf{x}) | \Phi \rangle = - \frac{e^2}{m} \mathbf{A} \langle \hat{n} \rangle . \quad (14)$$

where the flux density is proportional to the vector potential \mathbf{A} and the product $\hat{\psi}^\dagger(\mathbf{x}) \hat{\psi}(\mathbf{x})$, representing the particle density. In reality the vector potential influences the electron wave functions and the expression in brackets \mathbf{j}_1 contributes. For \mathbf{j}_1 to still vanish even though a magnetic field is switched on the electron wave functions need to be rigid, i.e. they must not change if a magnetic field is present. This rigidity can be accomplished by separating the ground and the excited state with an energy gap, which needs to be overcome by the strength of the magnetic field. The theory of the energy gap has turned out to be very successful and will be verified by this experiment.

BCS theory

A microscopic explanation for superconductivity was found by Bardeen, Cooper and Schrieffer. This theory addresses the following experimental findings:

1. Superconductivity vanishes for a critical temperature T_C , a critical current I_C or a critical magnetic field B_C .
2. The magnetic flux is quantised by $h/(2e)$.
3. The isotope effect, i.e. the critical temperature depends on the mass of the lattice particles $T_C \sim 1/\sqrt{m}$.
4. Ground and excited state are separated by an energy gap.

We just address these points right away. From 2. follows that electron pairs are responsible for charge transport and from 3. we conclude that the interaction is phononic.

For an attractive interaction between two electrons the ground state of the Fermi gas is no longer stable and the energy of those two electrons is lowered. How can such an attractive interaction arise?

This question was answered by Fröhlich in 1950 as he derived an interaction between electrons and phonons in terms of quantum field theory. The Hamiltonian of the whole system of electrons and phonons can be split into two independent parts of dynamics and interactions

$$H = H_0 + H_{\text{int}} . \quad (15)$$

The components read

$$H_0 = \sum_{\mathbf{k}, \sigma} \hbar \varepsilon_{\mathbf{k}} a_{\mathbf{k}, \sigma}^\dagger a_{\mathbf{k}, \sigma} + \sum_{\mathbf{w}, \sigma} \hbar \omega_{\mathbf{w}} b_{\mathbf{w}, \sigma}^\dagger b_{\mathbf{w}, \sigma} , \quad (16)$$

$$H_{\text{int}} = \hbar \sum_{\mathbf{k}, \mathbf{w}, \sigma} \left(g_{\mathbf{w}} b_{\mathbf{w}} a_{\mathbf{k}+\mathbf{w}, \sigma}^\dagger a_{\mathbf{k}, \sigma} + g_{\mathbf{w}}^* b_{\mathbf{w}}^\dagger a_{\mathbf{k}, \sigma}^\dagger a_{\mathbf{k}+\mathbf{w}, \sigma} \right) . \quad (17)$$

with coupling constants $g_{\mathbf{w}}$. We assumed that the interaction of the electron with the phonons does not alter the electron spin. Now the Hamiltonian is transformed into the Heisenberg picture where all initially time-independent operators are replaced by their time-dependent counterparts, which is denoted by a tilde. The Heisenberg equation of motion for the phonon creation operator reads

$$\dot{\tilde{b}}_{\mathbf{w}}^\dagger = \frac{i}{\hbar} [\tilde{H}, \tilde{b}_{\mathbf{w}}^\dagger] = i \sum_{\mathbf{k}, \sigma} g_{\mathbf{w}} e^{i(\varepsilon_{\mathbf{k}+\mathbf{w}} - \varepsilon_{\mathbf{k}} - \omega_{\mathbf{w}})t} \tilde{a}_{\mathbf{k}+\mathbf{w}, \sigma}^\dagger \tilde{a}_{\mathbf{k}, \sigma} . \quad (18)$$

If the operators were classical amplitudes, this would mean that the phonon amplitude changes depending on the electron movement. Intuitively one could say that an electron moving through the lattice polarises it by

deflecting the ions from their position of rest. This ion displacement influences the movement of the electrons in return. We consider a general operator \tilde{A} , which is made up of electron operators and write down its Heisenberg equation of motion

$$\dot{\tilde{A}} = i \sum_{\mathbf{k}, \mathbf{w}, \sigma} \left(g_{\mathbf{w}} [\tilde{a}_{\mathbf{k}+\mathbf{w}, \sigma}^\dagger \tilde{a}_{\mathbf{k}, \sigma}, \tilde{A}] \tilde{b}_{\mathbf{w}} e^{i(\varepsilon_{\mathbf{k}+\mathbf{w}} - \varepsilon_{\mathbf{k}} - \omega_{\mathbf{w}})t} + g_{\mathbf{w}}^* \tilde{b}_{\mathbf{w}}^\dagger [\tilde{a}_{\mathbf{k}, \sigma}^\dagger \tilde{a}_{\mathbf{k}+\mathbf{w}, \sigma}, \tilde{A}] e^{-i(\varepsilon_{\mathbf{k}+\mathbf{w}} - \varepsilon_{\mathbf{k}} - \omega_{\mathbf{w}})t} \right). \quad (19)$$

We integrate the equation of motion for $\tilde{b}_{\mathbf{w}}^\dagger$, assuming that the interaction of electrons and phonons is weak such that we can keep $\tilde{a}_{\mathbf{k}+\mathbf{w}, \sigma}^\dagger \tilde{a}_{\mathbf{k}, \sigma}$ constant in the temporal integration. We plug the result for $\tilde{b}_{\mathbf{w}}^\dagger$ into the equation of motion for \tilde{A} . After longish calculations and a back transform into the Schrödinger picture one can identify

$$\dot{\tilde{A}} = \frac{i}{\hbar} [H_0, \tilde{A}] + \frac{i}{\hbar} [H_{\text{int}}^{\text{eff}}, \tilde{A}] \quad (20)$$

in the equation of motion. For the effective interaction one has

$$H_{\text{int}}^{\text{eff}} = \hbar \sum_{\substack{\mathbf{k}, \mathbf{k}', \mathbf{w} \\ \sigma, \sigma'}} |g_{\mathbf{w}}|^2 \frac{\omega_{\mathbf{w}}}{(\varepsilon_{\mathbf{k}'+\mathbf{w}} - \varepsilon_{\mathbf{k}'})^2 - \omega_{\mathbf{w}}^2} \times a_{\mathbf{k}+\mathbf{w}, \sigma}^\dagger a_{\mathbf{k}', \sigma'}^\dagger a_{\mathbf{k}'+\mathbf{w}, \sigma'} a_{\mathbf{k}, \sigma} + \hbar \sum_{\mathbf{k}, \sigma} a_{\mathbf{k}, \sigma}^\dagger a_{\mathbf{k}, \sigma} \left[\sum_{\mathbf{w}} |g_{\mathbf{w}}|^2 \frac{1}{\varepsilon_{\mathbf{k}} - \varepsilon_{\mathbf{k}-\mathbf{w}} - \omega_{\mathbf{w}}} \right]. \quad (21)$$

The second term represents the self energy of the electron in the lattice, expressed by an energy shift, which can be accounted for with the effective mass. The first term includes the electron-electron interaction. This can be rewritten to

$$H_{\text{El-El}} = -\frac{1}{2} \sum_{\substack{\mathbf{k}, \mathbf{k}', \mathbf{w} \\ \sigma, \sigma'}} v_{\mathbf{k}, \mathbf{k}', \mathbf{w}} a_{\mathbf{k}+\mathbf{w}, \sigma}^\dagger a_{\mathbf{k}', \sigma'}^\dagger a_{\mathbf{k}'+\mathbf{w}, \sigma'} a_{\mathbf{k}, \sigma} \quad (22)$$

With this we can write down the Hamiltonian of superconductivity

$$H = \sum_{\mathbf{k}, \sigma} E_{\mathbf{k}} a_{\mathbf{k}, \sigma}^\dagger a_{\mathbf{k}, \sigma} - \frac{1}{2} \sum_{\substack{\mathbf{k}, \mathbf{k}', \mathbf{w} \\ \sigma, \sigma'}} v_{\mathbf{k}, \mathbf{k}', \mathbf{w}} a_{\mathbf{k}+\mathbf{w}, \sigma}^\dagger a_{\mathbf{k}', \sigma'}^\dagger a_{\mathbf{k}'+\mathbf{w}, \sigma'} a_{\mathbf{k}, \sigma}. \quad (23)$$

It is no longer obvious that the electron-electron interaction is actually mediated by a phonon. In 1956 Cooper found that even for this kind of Hamiltonian an attracting force between two electrons of opposite spin is possible. Thus we make up the states by creating pairs with opposite spin an wave vector from the vacuum state

$$\Phi = \prod_{\mathbf{k}} (u_{\mathbf{k}} + v_{\mathbf{k}} a_{\mathbf{k}, \uparrow}^\dagger a_{-\mathbf{k}, \downarrow}^\dagger) \Phi_0. \quad (24)$$

The derivation of this state is not trivial at all, cf. [1, 281–289]. In this reference the expectation value of the Hamiltonian with respect to Φ is also calculated. It reads

$$E = 2 \sum_{\mathbf{k}} E_{\mathbf{k}}' v_{\mathbf{k}}^2 - \sum_{\mathbf{k}, \mathbf{k}'} V_{\mathbf{k}, \mathbf{k}'} u_{\mathbf{k}} v_{\mathbf{k}} u_{\mathbf{k}'} v_{\mathbf{k}'} \quad (25)$$

with the abbreviation $2V_{\mathbf{k}, \mathbf{k}'} = (v_{\mathbf{k}, -\mathbf{k}', \mathbf{k}' - \mathbf{k}} + v_{-\mathbf{k}, \mathbf{k}', \mathbf{k} - \mathbf{k}'})$. Minimising the expectation value leads to an equation for the energy gap which solution is approximately given by

$$\Delta \approx 2\hbar\omega e^{-2/(D(E_F)V_0)} \quad (26)$$

with the density of states $D(E)$ of the electrons and the constant approximation of the matrix element of the interaction $V_{\mathbf{k}, \mathbf{k}'} = V_0$.

Types of Superconductors

Type I: A type I superconductor possesses a superconducting phase below the critical temperature. The magnetic field penetrates the material up to the London penetration depth and decays exponentially in that region. If the external magnetic field is raised too high the material performs a phase transition to the normal conducting phase.

Type II: In contrast to type I superconductors these materials do not immediately switch back to normal conduction when the external field is raised but go to an intermediate phase. In this state the magnetic field floods the conductor in form of quantised “flux sleeves”.

Josephson Effect

As the Cooper pairs, which are responsible for superconductivity are bosons they can condense into a common ground state which can be expressed using a macroscopic wave function like for a Bose-Einstein condensate. The macroscopic wave function of the BCS ground state reads

$$\psi = \psi_0 e^{i\varphi(r)} = \sqrt{n_S} e^{i\varphi(r)}, \quad (27)$$

with

$$\psi\psi^* = |\psi_0|^2 = n_S \quad (28)$$

The function $\varphi(r)$ denotes a phase and possesses a well-defined value for macroscopic distances. If we bring two superconductors close together, i.e. they are separated by an insulator of thickness less than 1 nm, the wave function of one superconductor can extend into the other. If the superconductors are separated farther they fulfil separate Schrödinger equations

$$i\hbar\dot{\psi}_1 = H_1\psi_1, \quad (29)$$

$$i\hbar\dot{\psi}_2 = H_2\psi_2. \quad (30)$$

with the eigenvalues E_1 and E_2 . For coupled superconductors we apply perturbation theory

$$\begin{aligned} i\hbar\dot{\psi}_1 &= E_1\psi_1 + \kappa\psi_2 \\ i\hbar\dot{\psi}_2 &= E_2\psi_2 + \kappa\psi_1 \end{aligned} \quad (31)$$

with the coupling parameter κ . In case of the superconductors comprising the same materials one has $n_{S1} = n_{S2} = n_S$ and $E_1 = E_2$ [2, p. 478]. If voltage drops at the junction we find

$$E_2 - E_1 = -2eU \quad (32)$$

We plug (27) into (31) and assume an explicit time dependency of the density n_S and the phase φ . Splitting real and imaginary part yields

$$\dot{n}_{S1} = \frac{2\kappa}{\hbar} \sqrt{n_{S1}n_{S2}} \sin(\varphi_2 - \varphi_1), \quad (33)$$

$$\dot{n}_{S2} = -\frac{2\kappa}{\hbar} \sqrt{n_{S1}n_{S2}} \sin(\varphi_2 - \varphi_1),$$

$$\dot{\varphi}_1 = \frac{\kappa}{\hbar} \sqrt{\frac{n_{S1}}{n_{S2}}} \cos(\varphi_2 - \varphi_1) - \frac{E_1}{\hbar}, \quad (34)$$

$$\dot{\varphi}_2 = \frac{\kappa}{\hbar} \sqrt{\frac{n_{S1}}{n_{S2}}} \cos(\varphi_2 - \varphi_1) + \frac{E_2}{\hbar}.$$

The difference of the latter two equations is

$$\hbar(\dot{\varphi}_2 - \dot{\varphi}_1) = -(E_2 - E_1) = 2eU \quad (35)$$

which is called the 1. Josephson equation.

If no voltage is applied to the tunneling junctions one has

$$\hbar(\dot{\varphi}_1 - \dot{\varphi}_2) = 0. \quad (36)$$

It follows immediately

$$\varphi_1 - \varphi_2 = \text{const}. \quad (37)$$

This implies constant arguments of the angular functions in (33) and thus

$$\dot{n}_{S1} = -\dot{n}_{S2}. \quad (38)$$

A current should flow between the two superconductors where n_{S1} and n_{S2} are constant, else the superconductors would get charged.

$$j_S = j_c \sin(\varphi_2 - \varphi_1) \quad (39)$$

is the 2. Josephson equation. A direct current flows between the two superconductors, but there is no voltage drop. This is called the direct current Josephson effect. The critical current j_c depends on the density of the Cooper pairs n_S , the contact area A and κ .

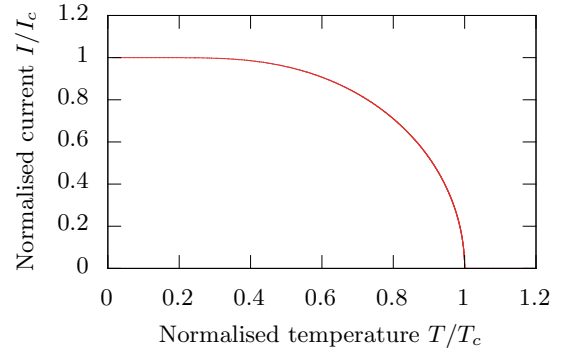


FIG. 1. Temperature dependence of the critical current. The red line is the isosurface where $I = I_c$. Below lies the superconducting phase, the normal conducting above.

Temperature and Magnetic Field Dependency

The BCS-theory implies a certain temperature dependence of the maximal Josephson current, which depends on the also temperature dependent energy gap $\Delta(T)$. The functional form of this dependency reads

$$I_c(T) = \frac{\pi\Delta(T)}{2eR} \tanh\left(\frac{\Delta(T)}{2k_B T}\right) \quad (40)$$

with the tunneling resistance R of the junction. A schematic graph is shown in figure 1.

For an insulator of thickness D the magnetic field is able to penetrate by λ_L . The effective thickness of the barrier is thus $d = 2\lambda_L + D$. The Ginzburg-Landau theory predicts for the phase at the junction

$$\varphi_2 - \varphi_1 = \frac{2\pi}{\phi_0} Bdx + \delta_0. \quad (41)$$

Plugging this into the 1. Josephson equation yields

$$j_S = j_c \sin\left(\frac{2\pi}{\phi_0} Bdx + \delta_0\right). \quad (42)$$

To obtain the whole current passing through the junction we need to integrate the current density over the surface A of the junction.

$$\begin{aligned} I_S(B) &= \int_A j_s(x) dA = \int_0^a dx \int_0^b dy j_s(x) \\ &= j_c A \sin\left(\frac{\pi}{\phi_0} Bda + \delta_0\right) \text{sinc}\left(\frac{Bda}{\phi_0}\right). \end{aligned} \quad (43)$$

The modulus of this maximal Josephson current is similar to the refraction on a slit.

$$I_c(B) = I_c(0) \left| \text{sinc}\left(\frac{Bda}{\phi_0}\right) \right|. \quad (44)$$

A schematic curve is depicted in figure 2.

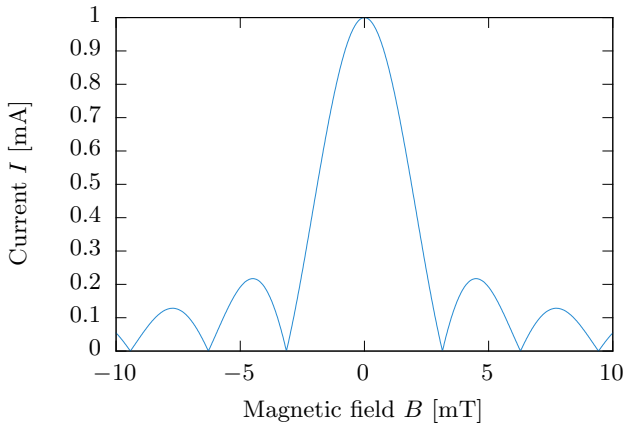


FIG. 2. Magnetic field dependence of the critical current.

ANALYSIS

Experimental Task

The experiment is mainly divided into three experimental tasks.

Current-Voltage Characteristic: In the first experimental task some I - U characteristics of the Josephson Junction are recorded. In the experimental setup there are four Josephson Junctions where two of them are shunted and the other two are not shunted. The characteristics are recorded with hysteresis and without. With help of the measured data it is then possible to discuss and determine the shuntresistance and the energy gap and the McCumber parameter.

Magnetic Field Dependency: To investigate the dependency of the magnetic field on the Josephson current I_C we use a Josephson Junction without hysteresis and measure the maximal Josephson current I_C for different coil currents of the Helmholtz coils. The corresponding magnetic field is given by

$$B = \left(\frac{4}{5}\right)^{3/2} \frac{\mu_0 n I}{R}, \quad (45)$$

where the ration n/R is given by $n/R = 2144 \text{ W dg m}^{-1}$ the calculation of the magnetic field B was done by LabVIEW during the experiment. By doing this, we can determine the London penetration depth λ_L and compare the experimental results with the theoretical description.

Temperature Dependency: The temperature of the Josephson Junction can be varied with an external voltage supply. By recording whole I - U characteristics for different temperatures it is possible to plot the maximal Josephson current as function of the temperature and compare the experimental data with the theoretical description. Furthermore we can determine the energy gap.

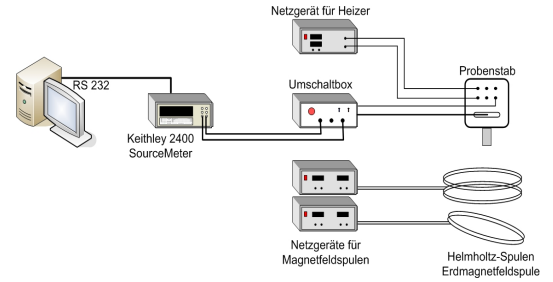


FIG. 3. Schematic illustration of the experimental setup.

The whole experimental setup is depicted in figure 3. As shown additional coils are used to compensate the earth magnetic field. With the Helmholtz coils it is possible to investigate the dependency of the Josephson current on the magnetic field. All measurements were done with help of LabVIEW.

Current-Voltage Characteristic

Hysteresis and Shuntresistance: As aforementioned the measurements were done and the Josephson current I_C is depicted as function of the voltage. In the case of the hysteresis the results are depicted in figure 4 (a).

A measurement without hysteresis is depicted in figure 4 (b). At $U = 0 \text{ V}$ there is a nonvanishing current I_C . As mentioned in the basics this corresponds with the theoretical description of the current free Josephson effect. As predicted at a critical current I_C the characteristic follows the well known linear Ohm characteristic. At this point all Cooper-pairs get broken and a tunneling process is not possible anymore. For higher voltage there is an additional irregularity.

The depicted behaviour indicates a shuntresistance parallel to the Josephson Junction. For voltages higher than the critical point only single electron current through the shuntresistance is possible. For high voltages the slope of the characteristic is therefore given by the parallel resistances of the normal conductor and the shuntresistance.

The subsequent measurements were done without hysteresis which is why an explicit discussion in the case of the hysteresis is not given here.

Maximal Josephson Current: To determine the maximal Josephson current I_C we use the enlarged measurements without hysteresis depicted in figure 5 (a). With help of the three depicted linear fits F_i it is possible to calculate I_C . The maximal Josephson current is given by half the difference of the intersection point of F_∞ and F_2 and the intersection point of F_2 and F_3 . If we use the

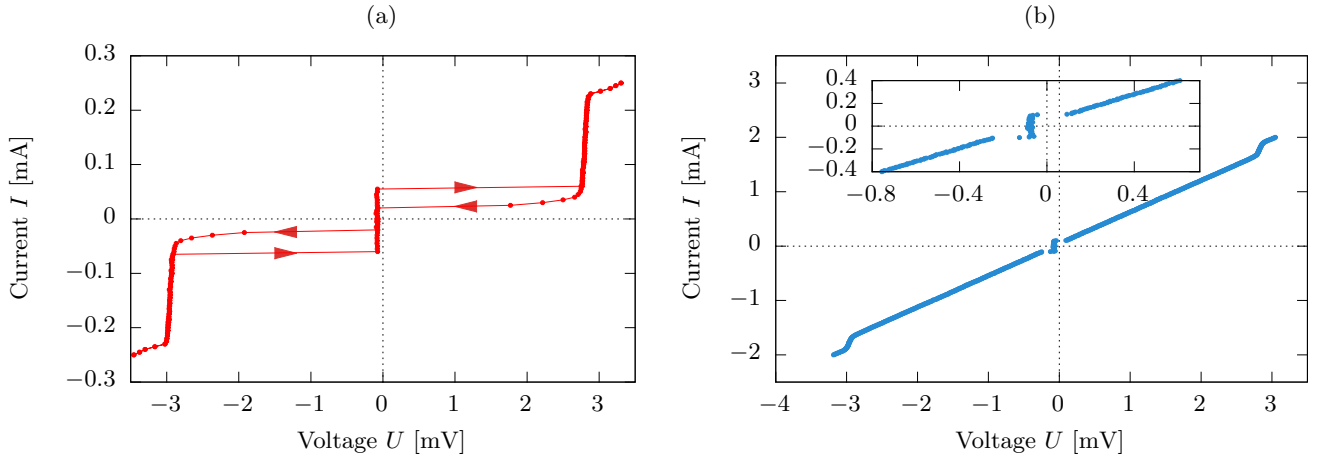


FIG. 4. From left to right: (a) Measured data with hysteresis. Shown is the measured current as function of the voltage. (b) Measured data with no hysteresis. For better visibility an inset is depicted in the top left corner.

notation

$$\mathcal{F}_1(U) = a_1 \cdot U + a_2, \quad (46)$$

$$\mathcal{F}_2(U) = b_1 \cdot U + b_2, \quad (47)$$

$$\mathcal{F}_3(U) = c_1 \cdot U + c_2, \quad (48)$$

it is easily to find

$$I_C = \frac{\mathcal{F}_1(U_1) - \mathcal{F}_2(U_2)}{2}, \quad (49)$$

where the voltages U_1 and U_2 are given by

$$U_1 = \frac{a_2 - b_2}{b_1 - a_1}, \quad U_2 = \frac{c_2 - b_2}{b_1 - c_1}. \quad (50)$$

Using the open source program gnuplot then leads to the maximal possible Josephson current

$$I_C = \frac{b_1}{2} \left(\frac{a_2 - b_2}{b_1 - a_1} - \frac{c_2 - b_2}{b_1 - c_1} \right) \quad (51)$$

$$= 0.097 \text{ mA}. \quad (52)$$

Energy Gap: Using the aforementioned calculations and fits to figure 5 (b) also allows the extraction of the size of the energy gap. The calculation is the same as above and one finds

$$2\Delta = U_g \cdot e, \quad (53)$$

where the voltage U_g is given by

$$U_g = \frac{1}{2} \left(\frac{b_1 - c_1}{c_2 - b_2} + \frac{b_1 - a_1}{a_2 - b_2} \right). \quad (54)$$

The difference between the previous calculation is the plus sign because now we want to calculate the mean value. With gnuplot we find

$$U_g = 2.823 \text{ mV}, \quad (55)$$

$$\Delta = 1.412 \text{ eV}, \quad (56)$$

where Δ is the energy gap.

Steward McCumber parameter: To determine the Steward McCumber parameter β_C we use the measurements without hysteresis depicted in figure 6. Using three linear fits

$$\mathcal{F}_1(U) = a_1 \cdot U + a_2, \quad (57)$$

$$\mathcal{F}_2(U) = b_1 \cdot U + b_2, \quad (58)$$

$$\mathcal{F}_3(U) = c_1 \cdot U + c_2, \quad (59)$$

and Ohms law $R = U \cdot I$ gives us the total resistance R_{tot}

$$R_{\text{tot}} = \frac{a_1 + b_1}{2}, \quad (60)$$

which is obviously the mean value. The shuntresistance is related to $R_S = c_1$. To determine the resistance of the normal conductor we use a simple parallel circuit of R_S and R_N , i.e. the total resistance is

$$\frac{1}{R_{\text{tot}}} = \frac{1}{R_N} + \frac{1}{R_S}. \quad (61)$$

A simple conversion leads to the resistance of the normal conductor

$$R_N = \left(\frac{1}{R_{\text{tot}}} - \frac{1}{R_S} \right)^{-1}. \quad (62)$$

With help of gnuplot we find

$$R_{\text{tot}} = 0.556 \Omega, \quad (63)$$

$$R_S = 0.584 \Omega, \quad (64)$$

$$R_N = 11.281 \Omega. \quad (65)$$

The McCumber parameter β_C is finally given by

$$\beta_C = \omega_P^2 R_{\text{tot}}^2 C^2 = \frac{2eI_C C}{\hbar} R_{\text{tot}}^2, \quad (66)$$

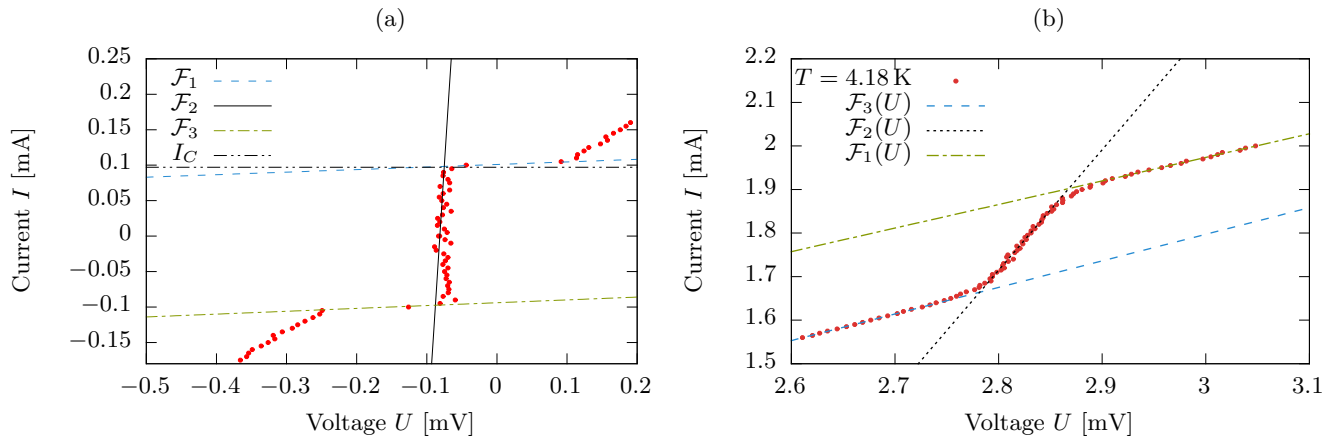


FIG. 5. From left to right: (a) Enlarged depiction of the critical Josephson Current I_C . The three linear fits \mathcal{F}_i are used to determine I_C . (b) Enlarged depiction of the bandgap with three linear fits to determine the gap voltage U_g and hence the energy gap Δ .

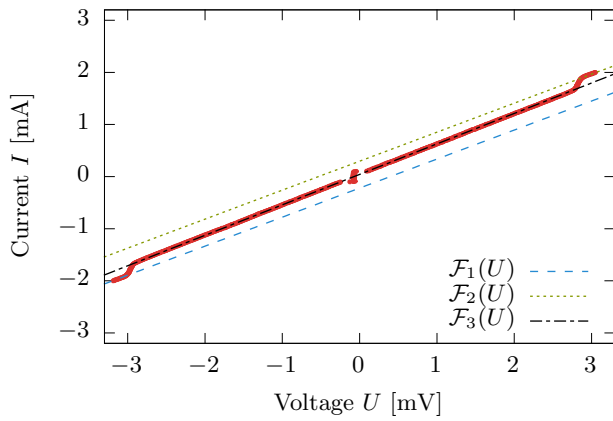


FIG. 6. Fits $\mathcal{F}_i(U)$ for the determination of the McCumber parameter β_C .

where the capacity C is 200 fF. Plugging all results in leads

$$\beta_C = 0.0182, \quad (67)$$

which is obviously much smaller than 1 and hence a hysteresis free junction. This result is not very astonishing because by just watching at the characteristic curve one can see this. Consequently the theoretical description and the experimental results are consistent.

Dependency of the Magnetic Field

In this section we want to discuss the dependency of the maximal Josephson current on an external magnetic field. To do so a lot of measurements had to be done. While varying the external magnetic field from 0.0 mT to 3.0 mT

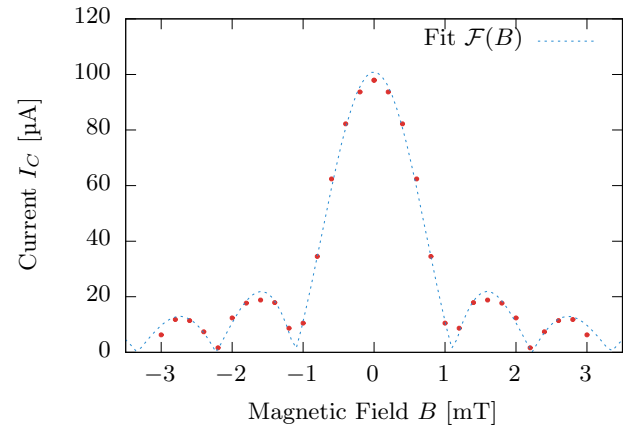


FIG. 7. Maximal Josephson current I_C as function of the magnetic field B .

in steps of 0.2 mT the characteristic curve were recorded and the maximal Josephson current I_C determined as describes above. The results are depicted in figure 7.

Note that the mirroring of the measured data is legal because of the symmetry of the expected diffraction pattern, i.e. only positive values of B had to be used.

To determine the London penetration depth λ_L it is necessary to use the fit function

$$\mathcal{F}(B) = a \cdot \left| \frac{\sin(b \cdot B)}{b \cdot B} \right|, \quad (68)$$

where the fit parameters are

$$a = 100.92 \mu\text{A}, \quad b = 2.823. \quad (69)$$

Here the fit parameter b is given by $b = \pi mT/B_\Delta$, where B_Δ denotes the distance of two minima of the diffraction pattern.

London Penetration Depth: Using the fit parameters a and b we can calculate the London penetration depth with

$$\lambda_L = \frac{1}{2} \left(\frac{b \cdot 10^3}{T} \cdot \frac{\hbar}{ew} - D \right), \quad (70)$$

where $D = 30$ nm is the thickness of the junction, e the elementary charge, \hbar the reduced Planck constant and $w = 10$ μ m the width of the junction. Plugging in all results leads

$$\lambda_L = 77.917 \text{ nm}. \quad (71)$$

Josephson Penetration Depth: Using the equation

$$\lambda_J = \sqrt{\frac{AwmT}{2\mu_0 I_C b}} \quad (72)$$

allows the calculation of the Josephson penetration depth λ_J . Here $A = 100$ μ m² is the surface of the Josephson Junction. Using $I_C = 97$ μ A (from above) and plugging in gives

$$\lambda_J = 38.12 \text{ } \mu\text{m}. \quad (73)$$

Obviously the condition $\lambda_J > w$ is fulfilled, i.e. the field induced by the supra currents can be neglected (see basics). Moreover we are not expecting a damping behaviour of the I_C - B curve depicted in figure 7.

The literature value for the London penetration depth of niobium is given by

$$\lambda_L^{\text{lit}} = 39 \text{ nm}. \quad (74)$$

Compared with our result of $\lambda_L = 77.917$ nm we achieve a percentage error of roughly $\delta\lambda_L \approx 50\%$ due to the purity of the sample.

Dependency of the Temperature

In the following section we want to discuss the dependence of different quantities on the temperature. Therefore we recorded the characteristic curve for the temperatures $T \in \{4.18 \text{ K}, 4.27 \text{ K}, 4.84 \text{ K}, 5.54 \text{ K}, 6.54 \text{ K}, 7.4 \text{ K}, 8.52 \text{ K}\}$. As discussed in the previous sections it is possible to find to each measurement the maximal Josephson current and the energy gap.

Maximal Josephson Current: The determined maximal Josephson currents as function of the temperature to each measurement are depicted in figure 8 (b). Figure 8 (a) shows the I - U characteristic near $U = 0$ for selected measurements. Both figures show a decreasing maximal Josephson current I_C for increasing temperature as predicted from the BCS theory. One finds the proportionality $I_C(T) \propto \tanh(T)$. To compare the experimental data with the theoretical expectations it is sensible to

transform to reduced quantities. To do so we introduce the reduced temperature T/T_C and a reduced energy gap $\Delta(T)/\Delta(0)$. It is then possible to convert the well known formula for the temperature dependence

$$I_C(T) = \frac{\pi}{2eR_N} \Delta(T) \tanh\left(\frac{\Delta(T)}{2k_B T}\right) \quad (75)$$

to a reduced formula

$$\frac{I_C(T)}{I_C(0)} = \frac{\Delta(T)}{\Delta(0)} \tanh\left(\frac{\Delta(T)}{2k_B T} \frac{T_C \Delta(0)}{T_C \Delta(0)}\right). \quad (76)$$

Let $x \equiv T/T_C$ and $y \equiv \Delta(T)/\Delta(0)$ be new variables, than we can write

$$\frac{I_C(T)}{I_C(0)} = y(x) \tanh\left(\frac{y(x)}{x} \frac{1.76}{2}\right). \quad (77)$$

This is an implicit function which is depicted in figure 8 (c). There are also the scaled data represented. To do so we have to divide the data by $I_C(0)$ or T_C . A possible assumption could be $I_C(0) \approx I_C(4.2 \text{ K}) = 97$ μ A (result from above) and the literature value $T_C = 9.2$ K. This case corresponds to the red dots in figure 8 (c). An optimisation for $I_C(0)$ and T_C leads to the parameters

$$T_C = 10.7 \text{ K}, \quad I_C(0) = 100 \text{ } \mu\text{A}. \quad (78)$$

Using these parameters gives the green dots depicted in the figure. The figure shows that our first assumption fits very well. Nevertheless we had to choose a higher critical temperature beyond that of niobium. This inconsistency is presumably based on the difficulty of measuring the real temperature at the Josephson Junction.

Energy Gap: Like in the previous chapter it is possible to calculate the energy gap by fitting the curves depicted in figure 8 (d). Note that in the figure are three selected measurements are depicted. In figure 8 (e) there are the results of the energy gap as function of the temperature. Obviously the energy gap decreases with increasing temperature. As done above it is possible to introduce reduced quantities. From the BCS theory we know the theoretical curve which we can rescale to

$$\frac{\Delta(T)}{\Delta(0)} = \tanh\left(\frac{T_C}{T} \frac{\Delta(T)}{\Delta(0)}\right), \quad (79)$$

where $\Delta(0) = 1.76k_B T_C$. Using the reduced variables $y \equiv \Delta(T)$ and $x \equiv T/T_C$ give birth to the implicit function

$$y(x) = \tanh\left(\frac{y(x)}{x}\right), \quad (80)$$

which is depicted in the reduced scheme in figure 8 (f). The red dots corresponds to the reduced energy gap values from figure 8 (e). For the scaling parameters we used the literature values $T_C = 0.2$ K and $2\Delta(0) = 2.9$ meV. The figure shows, that there is a remarkable correspondence between the experimental results and the theoretical predictions.

ERROR DISCUSSION

Due to the precision of the measuring devices and some technical limitations we want to discuss in this section typical sources of errors. The whole discussion is confined in a rather qualitative way than an explicit errors computation.

In all measurements and experimental tasks the measurement of the real temperature of the Josephson Junction was technically not possible. However, this problem was already mentioned in the instruction notes and approved in the analysis of the temperature dependence of I_C (see figure 8 (c)). Moreover the determination method of extracting the maximal Josephson current I_C especially for temperature near the critical temperatures seems to be unsuitable due to the small currents. Equally the determination of the energy gap $\Delta(T)$ is for temperatures near T_C nearly impossible. A more technical problem is the used software programme itself. From reasons we can not explain the programme often crashes, so we had to start the measurement process from the beginning.

SUMMARY

In this section we want to draw a short summary of the experimental results.

I-U Characteristic: In the first experimental task we measured the current-voltage characteristic for fix temperature $T = 4.2$ K with and without hysteresis. With help of a three linear fitting method the maximal Josephson current $I_C = 97 \mu\text{A}$ and the energy gap $\Delta = 1.412$ meV were calculated (see figure 5 (a) and (b)). Moreover it was possible to determine the shuntresistance $R_S = 0.585 \Omega$ as well as the normal conducting resistance. Note that we first calculated the total resistance and then with help of the formula of a simple parallel circuit the normal conducting resistance. Moreover we calculated the Steward McCumber parameter $\beta_C = 0.0182$ which is obviously much smaller than 1 and thus a overdamped Josephson Junction was used without hysteresis as depicted in figure 4 (b).

Dependency of the Magnetic Field: In the second tasks some characteristic curves were measured while varying the magnetic field. As predicted from the theory a typical diffraction pattern was measured which is shown in figure 7. With help of the measured data we calculated the London penetration depth $\lambda_L = 77.92$ nm and the Josephson penetration depth $\lambda_J = 38.12 \mu\text{m}$. Note that the Josephson penetration depth gives the typical length on which an external magnetic field penetrates into to Josephson Junction whereas the London penetration depth characterises the distance to which a magnetic field penetrates into a superconductor.

Dependency of the Temperature: In the last experimental task again some $I-U$ characteristics were measured

but this time for different temperatures. With help of the methods discussed in the previous experimental tasks it was then possible to calculate the maximal Josephson currents and energy gaps to each characteristic. The results are depicted in figure 8. Due to the known problem with the temperature measurement an optimisation of T_C and $I_C(0)$ in case of the dependency of the Josephson current on the temperature leads to

$$T_C = 10.7 \text{ K}, \quad I_C(0) = 100 \mu\text{A}, \quad (81)$$

which fits within the discussed errors to the theoretical prediction. Nevertheless the critical temperature is compared to the literature value of 9.2 K to high. Using reduced quantities in case of the dependency of the energy gap on the temperature as depicted in figure 8 (f) shows a remarkable correspondence between experimental results and the theoretical predictions.

* Michael.1233@gmx.de

† henrimenke@gmail.com

- [1] H. Haken, *Quantenfeldtheorie des Festkörpers*, 1st ed. (B.G. Teubner, 1973).
- [2] S. Hunklinger, *Festkörperphysik* (Oldenbourg Wissenschaftsverlag, 2007).

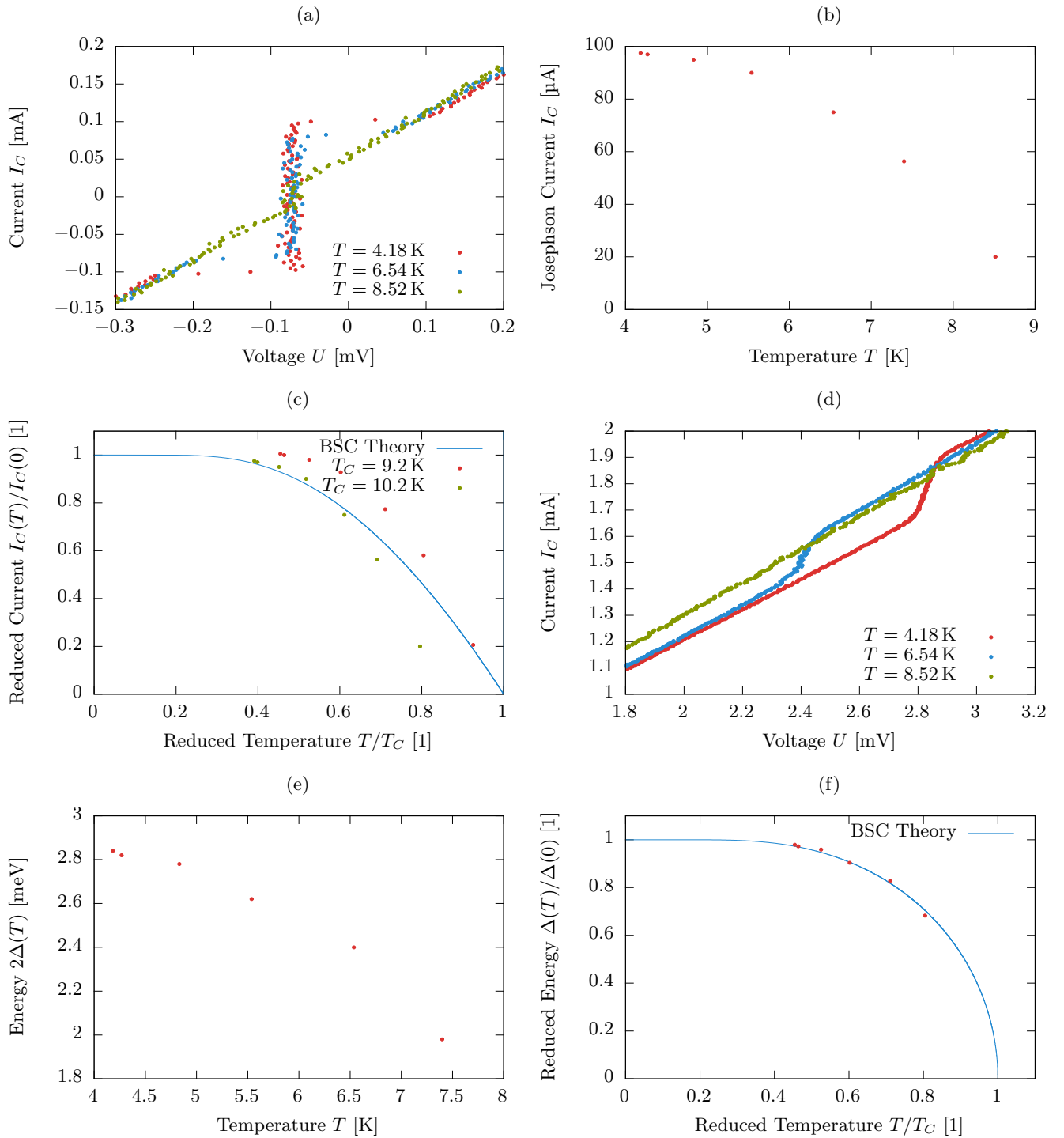


FIG. 8. From left to right: (a) Selected measurements near $U = 0$. For increasing temperature $T \rightarrow T_C$ the maximal Josephson current I_C decreases. (b) Maximum Josephson current I_C as function of the temperature T . (c) Reduced Josephson current as function of the reduced temperature. The blue line corresponds to the theoretical result of the BSC theory. The red dots corresponds to the literature value $T_C = 9.2$ K with $I_C = 97$ μ A as calculated in the previous tasks. The green dots results from the optimisation with $I_C(0) = 0.1$ μ A and a critical temperature of $T_C = 10.7$ K. (d) Selected measurements near $U = 2\Delta/e$. As predicted from the BSC theory the energy gap decreases for increasing temperature. (e) Dependence of the energy gap 2Δ on the temperature. (f) Reduced energy gap as function of the reduced temperature. The blue curve arises from the BSC theory. To calculate the reduced quantities we used the literature values $2\Delta(0) = 2.9$ meV and $T_C = 9.2$ K.